ON THE CANONICAL SHAPE OF SIMPLE CRATERS. E. Martellato[1], V. Vivaldi[1,2], G. Cremonese[1], M. Massironi[2], F. Marzari[3], M. Robinson[4], J. Haruyama[5], [1]INAF-Astronomical Observatory of Padova, Padova, Italy (elena.martellato@oapd.inaf.it); [2]Geoscience Dept., University of Padova, Padova, Italy; [3]Physics and Astronomy Dept., University of Padova, Padova, Italy; [4]SESE, Arizona State University, Tempe, Arizona, USA; [5]Solar System Science Division, ISAS, JAXA, Kanagawa, Japan

Introduction: Linné crater is located near the western edge of Mare Serenitatis (27.7°N, 11.8°E). Lunar Orbiter and Apollo missions provided the first images of the structure, revealing an apparent bowl-shaped cavity, surrounded by a circular raised rim and bright ejecta deposit. However, recent high-resolution data acquired by the Lunar Reconnaissance Orbiter Camera (LROC) onboard the NASA spacecraft Lunar Reconnaissance Orbiter (LRO) [1] revealed instead an inverted truncated cone shape for the crater [2]. In the past Linné crater was often used as an archetype for simple craters [3], a prime example of a simple fresh crater; We test the hypothesis that that this crater is indeed an archetype of this impact crater class (simple bowl shaped), and investigate its morphology in terms of target material properties.

Geological analysis: We investigated Linné crater and its surroundings with a suite of new remote sensing observations.

LRO data: Linné measures 2.220 km in diameter, and 0.543 km in depth, with d/D of 0.245. Its interior shape is best described as an inverted truncated cone, whose profile is best fitted by a truncated cone with a power law exponent n of 1.4-1.5, with a mean inner cavity wall slope of 33° [2]. The deposit on the crater floor is interpreted as a lens of breccia and impact melt with material that slumped down from the rim and crater walls (e.g., [4]).

We carried out morphometric analyses on the high resolution (sampled at 2 m spacing) LROC Digital Terrain Model (DTM) NAC_DTM_LINNECRATER_E280N0120. We tested different ranges of kernel sizes (15-35-50-75), in accordance with a multiscalar approach [5], in order to retrieve morphometric variables such as slope (first derivative) and curvatures (second derivatives). In Fig. 1, the stretching and the classification of the profile curvature highlighted the presence of three morphological steps below the rim crest. They are located at +50, -100, and -200 m depths respectively, with respect to the pre-impact surface, whereas the crater rim is about +100 m. The pre-impact surface is the reference for the numerical modelling, and corresponds to the absolute value -2630 m measured by LROC and the laser altimeter LOLA. Such morphological boundaries may represent near-surface volcanic layering (contacts between basaltic flow units).

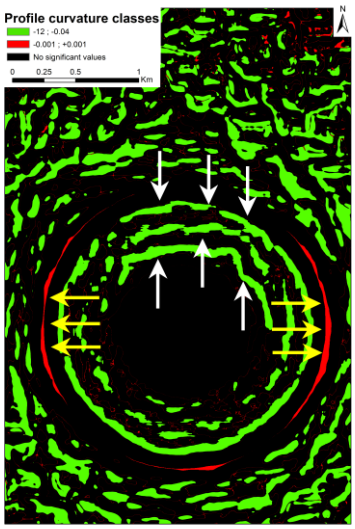

Figure 1: This image shows a specific classification of profile curvature derived from DTM. The red edge stands for the rim crest, whereas the green boundaries are representative of morphologic steps associated to the volcanic layering.

KAGUYA data: The Lunar Radar Sounder (LRS) onboard the Kaguya spacecraft (SELENE) probes the subsurface to a depth of several km with HF band (5 MHz; e.g., [6]). Our analyses of LRS data close to Linné crater (LRS_SWH_RV20_20071217103958) did not reveal any definitive subsurface boundaries. This finding might indicate the absence of layering, or it might suggest also that there is no regolith layer thick enough to echo the radar pulse [7].

Discussion: The different results derived by NAC DTM and microwave sensing can be balanced by considering Linné to form in a stack of lava flows with similar rheological behavior, which were emplaced shortly one after the other, preventing the accumulation of thick regolith deposits between the layers. We numerically modelled the formation of Linné crater to test the interpretation that the DTM reveals subsurface layering.

Methods: Numerical modelling was performed through the iSALE shock physics code. Initially developed by [8], the code has been enhanced through

modifications which include an elasto-plastic constitutive model, fragmentation models, various equations of state (EoS), multiple materials, a novel porosity compaction model, the ε-α-model [9, 10, 11, 12]. In addition, the code was tested against laboratory experiments at low and high strain-rates [12] and other hydrocodes [13].

The outcome from modelling is compared with the crater DTM (pixel scale 2 m), which was derived from LROC NAC stereo pairs and controlled to LOLA laser altimeter transects [14].

Results and Discussion: The models of Linné crater formation were obtained with a 38 m radius basaltic projectile (density ~ 2.8 g/cm^3) impacting at 18 km/s into a double-layered basaltic halfspace. We considered only two layers due to the rheological similarities observed in the geological analysis. The thermodynamic behavior of both the projectile and the target is described by tabular equation of states (ANEOS). The two layers are defined by either different strength or damage model. The upper layer is indeed assumed to be fractured.

Different thicknesses were considered for the upper fractured layer, in accordance with the values found in the morphometric analysis. At small thickness values, craters predominantly develop in the harder crustal material (thicknesses lower than 100 m). Higher the fractured layer thickness, more the crater forms in such upper weak layer. In the case of a 400-m thickness for the upper layer, the crater develops a bowl-shaped morphology and edgeless rims. As example, in Fig. 2 we report the model case for the 50-m fractured layer, for which a good fit was obtained with the DTM.

Linné crater, with its peculiar cone-truncated shape, remains the best example for simple craters.

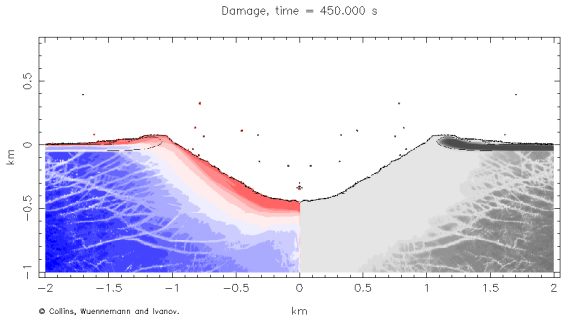

Figure 2. Final model crater obtained in the case of 50 m thickness upper fractured layer. Left side shows the Total Plastic Deformation (TPS, red: maximum deformation; blue: no deformation). On the left side, contours of the amount of damage are shown on a gray scale (white: maximum level of damage).

Future Work: In addition, to account for the variation in pre-impact crustal thickness, we are going to consider into our analysis the ejecta distribution. In our simulations, we have included Lagrangian tracer particles to track the position of the ejected mass. We will evaluate the final ejecta distribution by fitting the tracer data with a ballistic trajectory.

References: [1] Robinson M.S. et al. (2010) *Space Science Sci. Rev., 150*, 81-124. [2] Garvin J.B: et al. (2011) *LPS XLII*, Abstract # 2063. [3] Melosh H.J. (1989) Impact cratering: A geologic process. *New York: Oxford University Press*, 245 p. [4] Cintala M.J. and Grieve, R.A.F. (1998) *Meteoritics & Planet. Sci., 33*, 889-912. [5] Wood J. (1996) The geomorphological characterization of digital elevation models, *PhD Thesis*, University of Leicester, UK. [6] Ono T. and Oya H. (2000) *Earth Planets Space, 52*, 629-637. [7] Ono T. et al. (2009) *Science, 323*, 909-912. [8] Amsden A.A. et al. (1980) *Los Alamos National Laboratories*, Report LA–8095. [9] Collins G.S. et al. (2004) *Meteoritics & Planet. Sci., 39*, 217-231, 2004. [10] Ivanov B.A. et al. (1997) *Int. J. Impact Eng., 20*, 411-430. [11] Melosh H.J. et al. (1992) *JGR, 97*, 14,735-14,759. [12] Wünnemann K. et al. (2006) *Icarus, 180*, 514-527. [13] Pierazzo E. et al. (2008) *Meteoritics & Planet. Sci., 43*, 1917–1938. [14] Henriksen M.R. et al. (2014) *LPS XLV*, Abstract # 2851.

Acknowledgements: We gratefully acknowledge the developers of iSALE-2D, including G. Collins, K. Wünnemann, D. Elbeshausen, B.A. Ivanov and J. Melosh (www.iSALE-code.de).